

High Average Power S-Band Digital Phase Shifter

ROBERT AVERY MOORE, SENIOR MEMBER, IEEE, GUS M. KERN, MEMBER, IEEE, AND
LAWSON FRENCH COOPER, MEMBER, IEEE

Abstract—A 100-kW-peak 2-kW-average-power liquid-cooled ferrite digital phase shifter has been constructed using beryllia cooling of the ferrite toroid to meet single axis scanned array requirements. The phase-shift cross section external to the ferrite toroids is completely filled with the beryllia. Experiments indicate that the maximum temperature rise in the ferrite is no greater than 45°C. In tests using flux drive to 2 kW, the phase shifter exhibits a maximum phase drift of $\pm 6^\circ$ for 90° differential phase shift. The differential phase shift versus frequency varies less than $\pm 0.5^\circ$ for a 3-percent bandwidth.

I. INTRODUCTION

A N S-band phase shifter with a peak power capability of 100 kW and an average power capability of 2 kW has been constructed using garnet as the phase-shifter medium to meet single axis scanned array requirements. A literature review shows that this peak power was previously projected by Whicker and Jones [1] and exceeded by Rodrigue *et al.* [2]. Subsequent to this development, Stern and Agrios [3] have reported similar peak powers. Though materials were identified for each of these programs in the papers referenced, the only materials referenced which would provide the required peak power capability in the band of interest were in-house materials not available for the present project. A series of materials which were modifications of those commercially available were evaluated to identify a material which would meet the peak power requirement.

No one has reported an average power equivalent to 2 kW in a toroidal type latching ferrite phase shifter. The greatest average power previously reported at S-band is 900 W by Rodrigue *et al.* [2]. The problem in transmitting high average power is, of course, transmission of the heat out of the ferrite material due to the power absorbed by the material. Since garnet is a relatively poor conductor of heat, a much greater average power can be achieved by providing a low thermal resistance path from the broad face of the ferrite toroids to the waveguide walls. This was done in part by Rodrigue *et al.* [2, fig. 7] by means of a pair of boron nitride slabs and a pair of T's contacting the broad wall of the ferrite toroid [2]. Both of these techniques provided a substantial improvement over that attainable by the use of the ferrite toroids without a dielectric thermal path.

Achieving 2-kW average power required an improved thermal path. The design approach selected made use of ber-

yllia which has a thermal conductivity over four times that of boron nitride. Beryllia, however, has a dielectric constant of 7 while boron nitride has a dielectric constant of 4. (Beryllia also has the disadvantage of requiring special machining techniques because of its toxic effects and can only be machined by suitably equipped shops.) In addition, the total waveguide cross section external to the garnet was dielectric filled providing thereby an improved thermal path to the waveguide walls and simplifying the geometry relative to analysis. This geometry was programmed for computer design, such that the differential phase, as required by the application, is directly provided for in the design. The design described herein yielded a differential phase-shift variation of less than $\pm 0.5^\circ$ for a differential phase shift of 90° over a 3-percent frequency band.

II. LOW POWER CHARACTERISTICS

Although the selection of high power material was not available at the outset of the program, designing to meet RF parameters, i.e., differential phase shift, bandwidth, insertion loss, and VSWR, was done with the view toward meeting the power requirements. Essentially, this meant making concessions to selection of the material and thermal configuration in the design of these RF cross sections. A modified form of G-500, MS3516C, was developed to meet the peak power requirement. For approximate phase-shift characteristics, the properties of G-500 (published in the Trans Tech Catalog) were used [4]. The thermal design, illustrated in Fig. 1, makes use of a completely dielectric

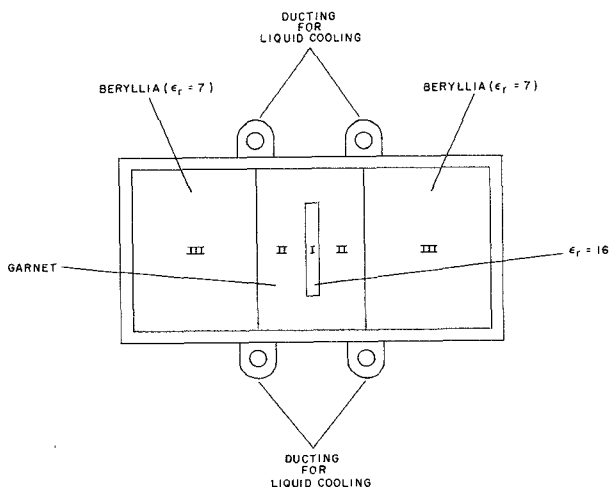


Fig. 1. Cross section of high average power phase shifter using beryllia dielectric loading for thermal path between garnet and waveguide walls.

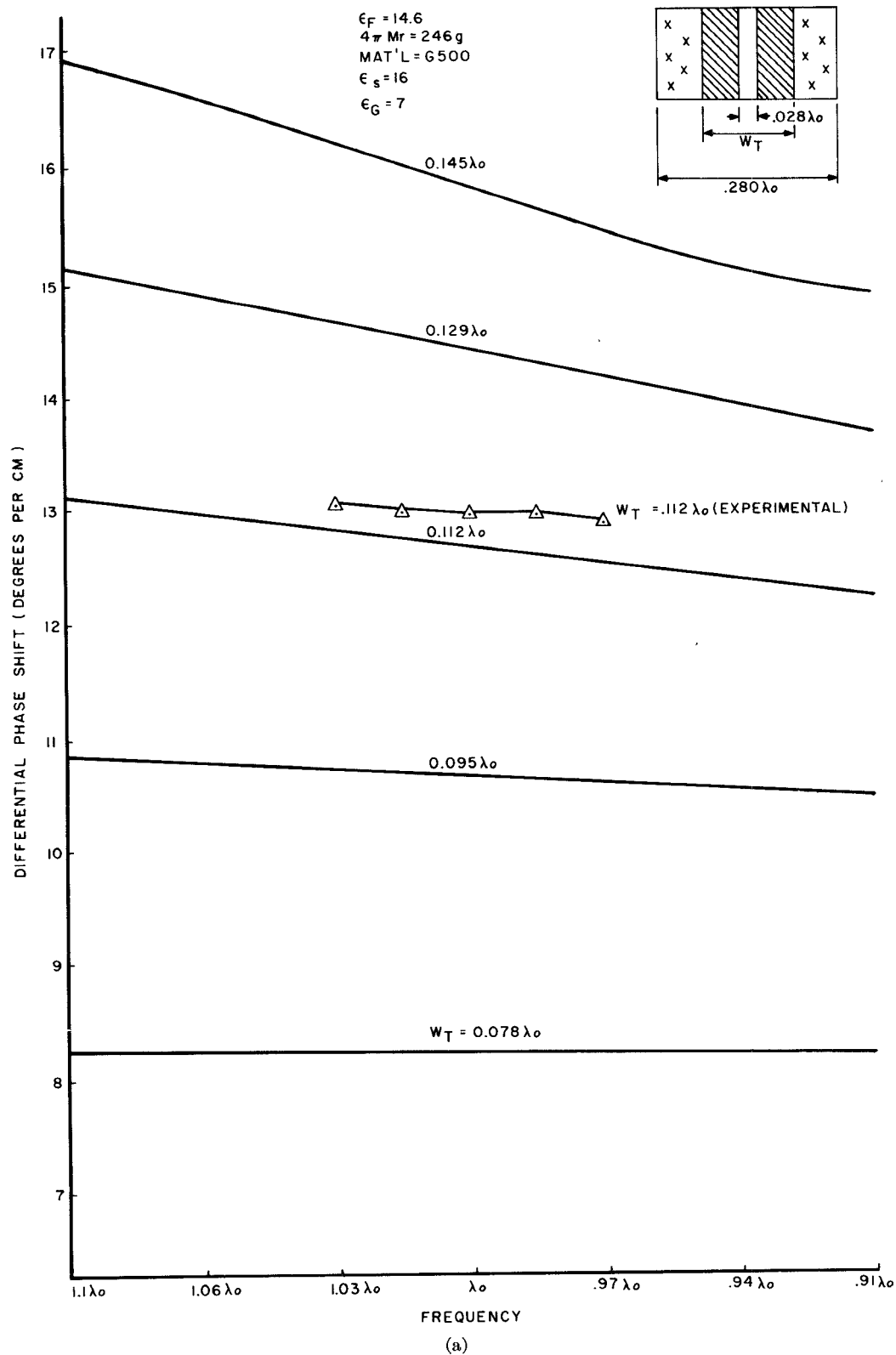


Fig. 2. (a) Computed and experimental differential phase shift as a function of relative wavenumbers for waveguide width at $0.280\lambda_0$. (b) Computed differential phase shift as a function of relative wavenumber for a waveguide at $0.350\lambda_0$. (c) Computed differential phase shift as a function of relative wavenumber for a waveguide width at $0.420\lambda_0$. (d) Computed differential phase shift as a function of relative wavenumber for a waveguide width at $0.560\lambda_0$.

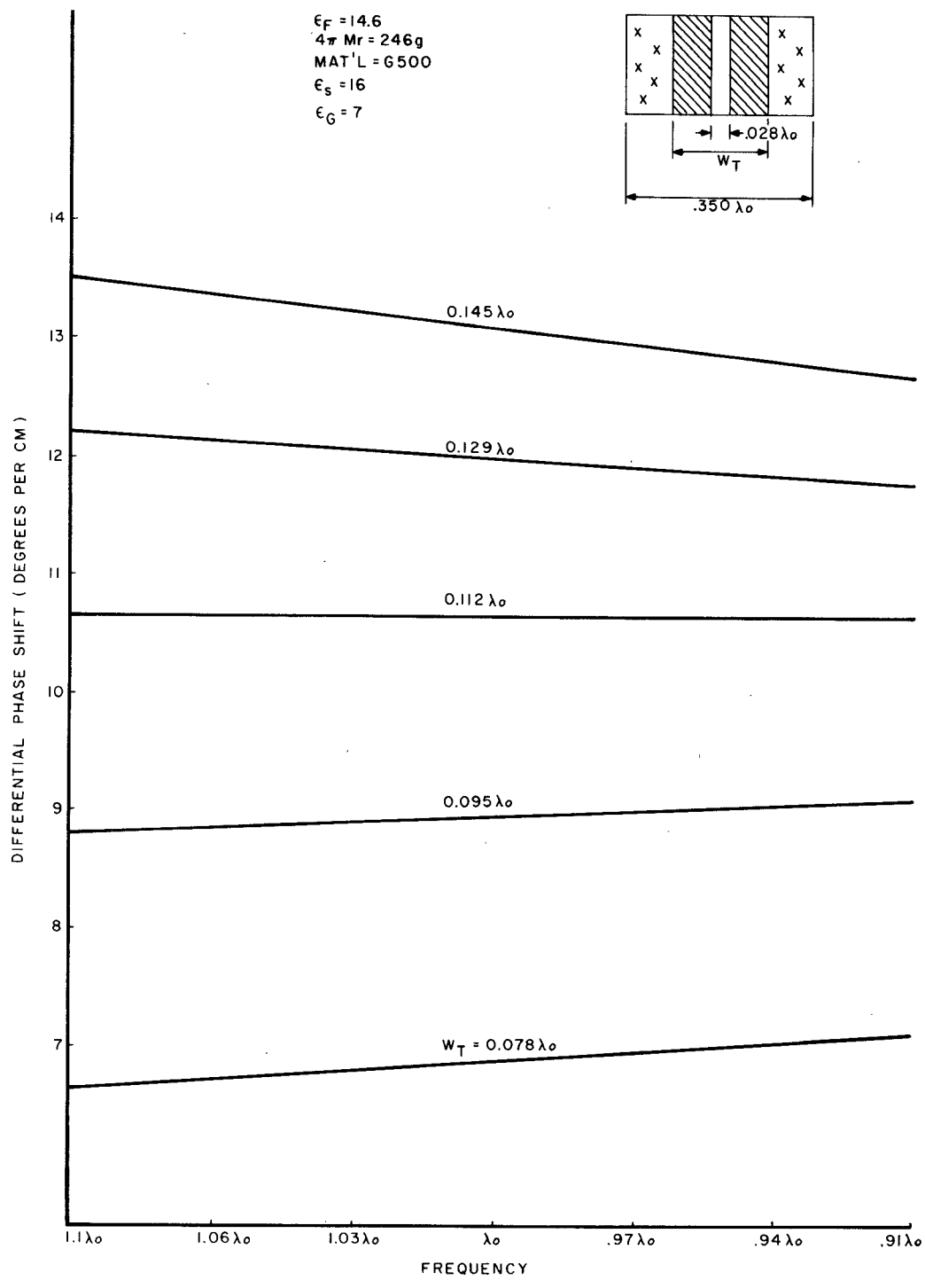


Fig. 2. (Continued.)

filled cross section. This configuration provides a minimum thermal resistance between the garnet toroid surface and the waveguide walls. An additional attraction is the admissibility of its phase-shift characteristics to computer design. The details of material selection and the thermal design are given in subsequent sections.

The exact RF cross section was established by a computer analysis based on the Ph.D. dissertation of Allen [5]. The characteristic equation was written to provide for a

separate dielectric in each of regions I, II, and III as shown in Fig. 1. With this formulation, differential phase shift as a function of transverse dimensions, dielectric constants, and ferrite remanent flux can be investigated. An investigation of phase shift as a function of these parameters was carried out. The most critical phase characteristics in carrying out the investigation were achieving constant differential phase shift as a function of frequency and maximum differential phase shift per unit length. It

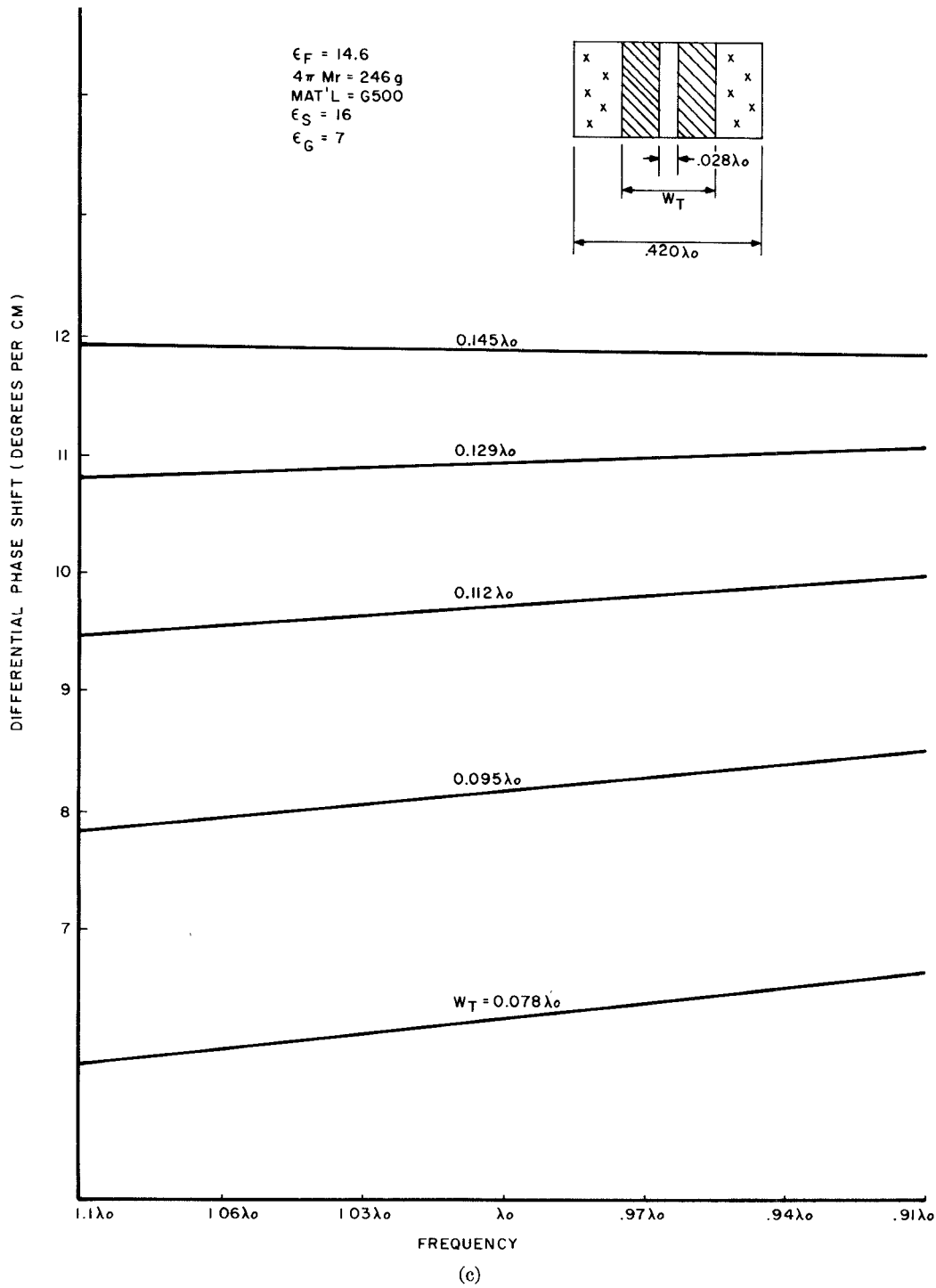


Fig. 2. (Continued.)

was also felt that the cross section should be sufficiently small to minimize the number of higher order modes which can propagate. Fig. 2(a)-(d) shows curves of differential phase versus normalized frequency for transverse dimension waveguide widths of $0.280\lambda_0$, $0.350\lambda_0$, $0.420\lambda_0$, and $0.560\lambda_0$ (λ_0 is centerband free space wavelength). The other dimensions and cross-sectional characteristics are shown on the figure. ϵ_G refers to the dielectric constant of the region between the ferrite and the waveguide walls. ϵ_S refers to the dielectric constant of the dielectric in the slot and ϵ_F to the dielectric constant of

the garnet. Normalized relative to a free space wavelength, these charts should give sufficient information for many design purposes at other frequencies. For the present problem, these curves were used to identify the combinations of parameters yielding maximum phase sensitivity for a flat phase shift versus frequency response.

With no effort made to determine the broadest possible band, the results show a constant differential phase versus normalized frequency for a 20-percent band at S band clearly indicating that dielectric loading of the region between the ferrite and the waveguide walls is compatible

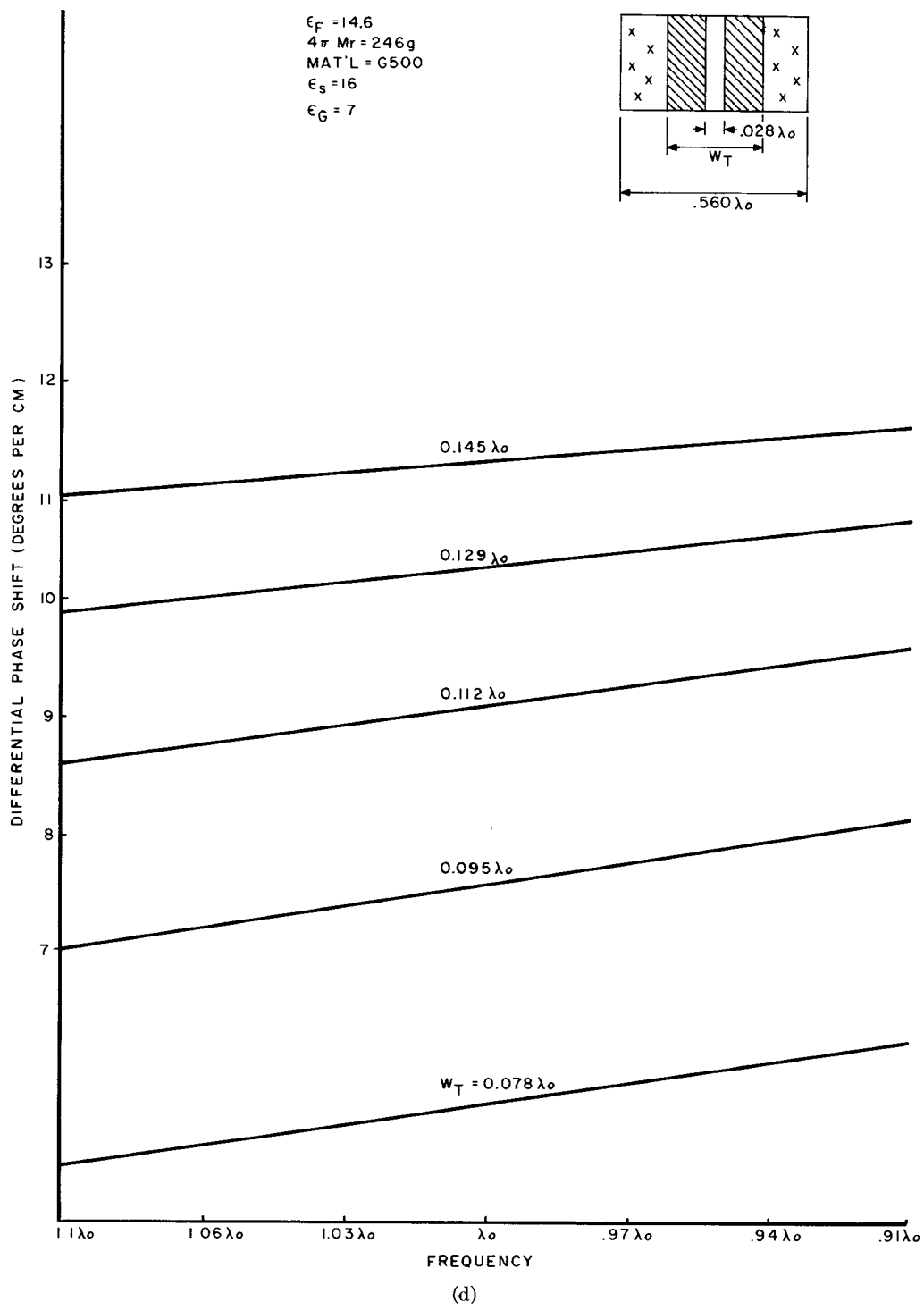


Fig. 2. (Continued.)

with achieving a flat phase shift versus frequency response and a high phase activity per unit length. To assure that substantial phase shift per unit length was not being sacrificed by virtue of the dielectric loading, the phase-shift characteristics were computed for the same toroid widths with the region between the ferrite and waveguide walls unloaded. This computation was carried out for a $0.560\lambda_0$ waveguide width. The result of this computation is shown in Fig. 3. This computation does not cover the complete range of parameters covered in Fig. 2, but a comparison

of phase shift per unit length for constant garnet widths (W_t) indicates that the phase activity of the loaded configuration (Fig. 2) is equal to or greater than the unloaded configuration (Fig. 3).

For the dielectric loaded configuration (Fig. 2) suitable for high average power, flat differential phase versus frequency is available for normalized waveguide widths between $0.280\lambda_0$ and $0.350\lambda_0$. It is also noticed that by accepting a slightly decreasing phase with frequency, a significantly greater phase shift per unit length is possible.

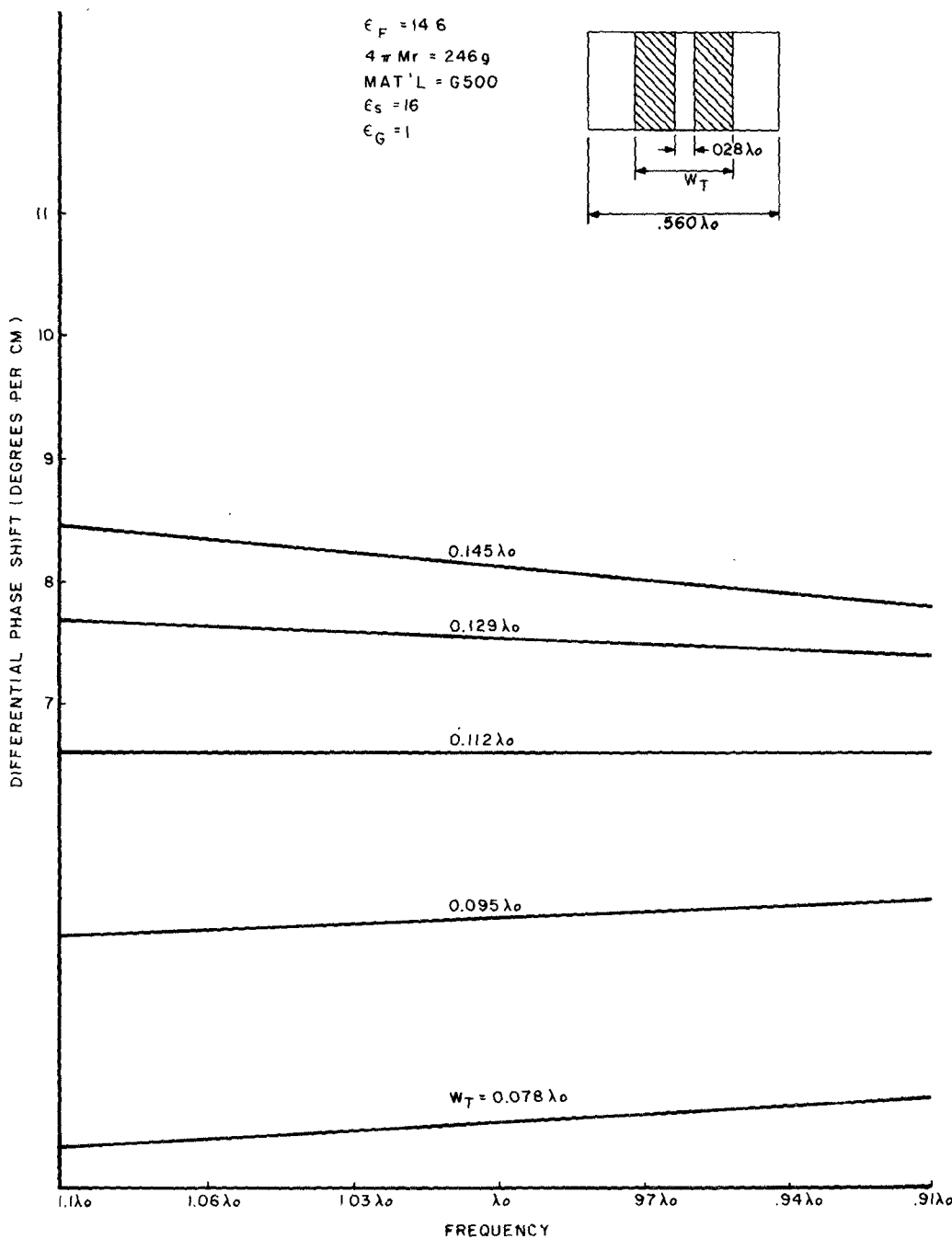


Fig. 3. Computed differential phase shift for $\epsilon_r = 1$ for regions between ferrite and waveguide walls for the waveguide width $0.560 \lambda_0$.

Accordingly, the inside waveguide width was chosen to be $0.280 \lambda_0$ with a ferrite toroid width of $0.11 \lambda_0$. For these dimensions the analysis predicts $13^\circ/\text{cm}$ differential phase shift.

The result of low power phase measurements of a phase shifter constructed to meet the above criteria and temperature stabilized at 25°C is shown in Fig. 2(a). The differential phase shift is slightly greater than that computed.

Insertion loss and VSWR of a 90° phase shifter are shown in Figs. 4 and 5. For the band of interest $0.97 \lambda_0$ – $1.03 \lambda_0$ the insertion loss is less than 0.5 dB , while the VSWR is less than 1.1 . The 0.5-dB insertion loss consists of the

loss of dielectric phase equalization sections as well as the ferrite–beryllia phase-shift structure. The insertion loss of the ferrite–dielectric structure is approximately 0.32 dB .

III. PEAK POWER

A series of materials were tested to determine one which would meet high peak power, provide an adequate phase shift per unit length, and minimize insertion loss. This tradeoff leads to the selection of the saturation moment and ΔH_K as a consequence of the selection of the material and required substitutes and dopings. The initial composition selected was based on the use of the chart of,

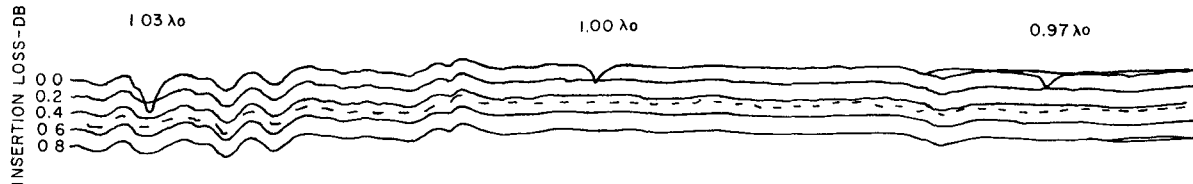


Fig. 4. Insertion loss of high average power phase shifter. Over the band of interest $1.03 \lambda_0$ – $0.97 \lambda_0$ the insertion loss is less than 0.5 dB.

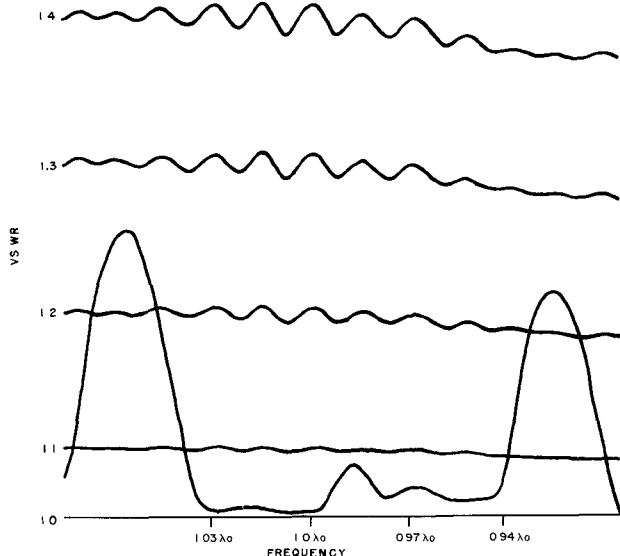


Fig. 5. Input VSWR versus frequency of high average power phase shifter. Over the band of interest $1.03 \lambda_0$ – $0.97 \lambda_0$ the VSWR is less than 1.1.

“Ferrite critical field dependence of magnetization” [2, fig. 6] versus saturation moment for a series of aluminum and gadolinium doped YIG ferrites. This suggested a material with a saturation moment of 500–600 G doped for a ΔH_K of 30–50 Oe. On this basis, Trans Tech G-500, G-600, and modified versions of these were peak power tested at an approximately 1- μ s pulse length in an epoxy-bonded precisely dimensioned dielectric loaded structure designed to meet the average power requirement. The structure consisted of transverse dielectric loading in the phase-shift section as well as longitudinal dielectric loading employed to equalize total phase length of individual phase shifters. Arc susceptibility was minimized through use of a precision waveguide housing and soft metal foil gasketing to obtain intimate top and bottom wall contact with the composite equalized phase length phase-shift structure.

The standard materials test results shown in Fig. 6 clearly indicate an increasing peak power capability with decreasing saturation moment. Increasing amounts of cerium and holmium as shown in Fig. 7 were added to G-500 to obtain the 3516 series of materials. The H_{co} curve for $K = 6$ Oe is appropriate for gadolinium–aluminum doped garnets, while the dashed curve shows the standard materials curve modified to indicate an approximate relationship between peak power and composition [6].

Neither arcing nor nonlinear saturation of MS 3516 C

was observed at peak power levels up to 150 kW during the course of this program. Tests conducted during a later program have established that nonlinearity for our geometry would occur at 190 kW. This corresponds to an h_{crit} of approximately 65 Oe. It should be noted that the H_{co} achieved in our experiments was similar to that of Killick though slightly higher H_{co} were achieved for the same level of holmium doping. A possible reason for this deviation is that Killick’s composition contained a greater ratio of metal oxides to rare earth oxides than is typical for aluminum substituted yttrium iron garnet. A second possible reason is the computation of H_{co} from the peak power level at which nonlinearity is observed. Since this is a very sensitive function of geometry, some deviation between differing geometries can occur here. Our value of H_{co} is calculated as a function of peak power at the point of nonlinearity using the Killick [6] relationship.

IV. AVERAGE POWER

The handling of high average power is essentially the task of minimizing the insertion loss (and thereby the heat generated by the high power) and achieving a minimum thermal resistance between the interior of the ferrite and the coolant. Liquid coolant maintained at 25°C was provided on the broad walls as shown in Fig. 1. Other techniques, such as the use of temperature compensated garnets and of flux drive, minimize the effect of temperature rise in the toroid. Both of these techniques were utilized. The material 3516C⁴ is a modified form of the Gd-Al-doped YIG garnet G-500 with a saturation moment between that of G-500 and G-600.

The flux drive used for the phase-shifter integrates the voltage across the latching wire and shuts off the drive at a predetermined level. Since the voltage across the latching wire is equal to the back EMF due to the changing flux, this integration leads to $(d\phi/d_t) d_t = \phi(t)$. The drive is shut off when the integral equals the predetermined value of $\phi(t_0)$ for the phase setting. This approach is effective to the extent the latching wire resistance drop is much less than $d\phi/d_t$, and the material is square loop so that the quiescent phase setting is equal to $\phi(t_0)$.

The thermal design provides for a minimum thermal resistance between the surface of the ferrite toroids and the waveguide walls. This overcomes, in so far as is possible, the difficulty of dissipating the heat generated in the ferrite but still leaves the problem of heat transmission from the interior of the toroid. The latter could be improved upon somewhat by the use of thinner toroids and

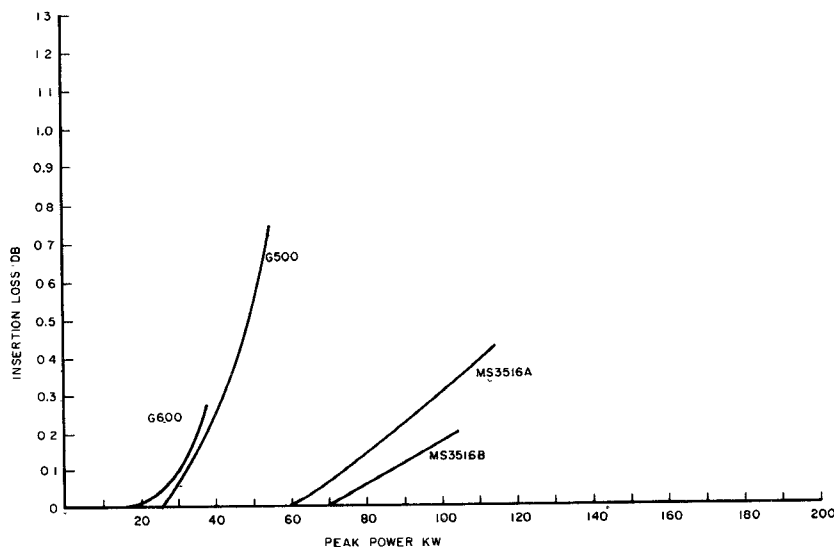


Fig. 6. Measurement of peak power saturation for a series of garnet materials tested toward meeting 100-kW peak power. Though the saturation point for MS3516C was not found, it is safely above 100 kW

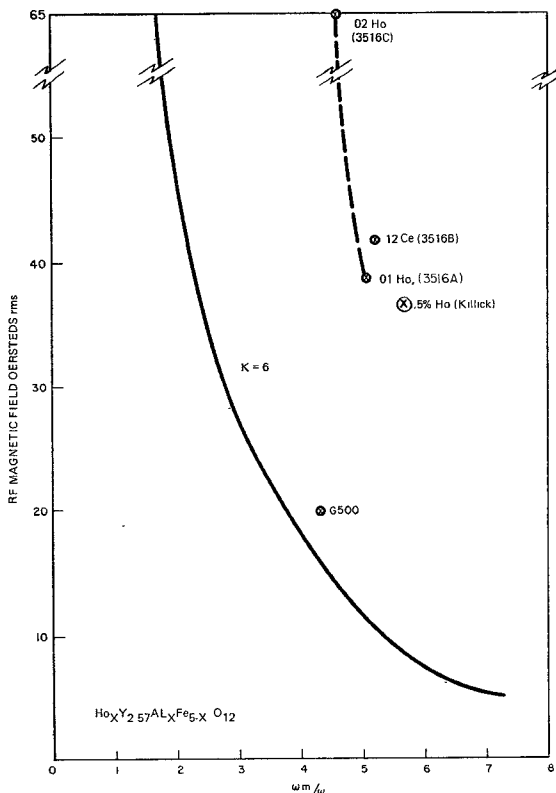


Fig. 7. Curves showing approximate relation of peak power and composition. Curve labeled $K = 6$ is based on formula $H_{co} = 2K((1/2.81Ms/f) - 1)$. The numerical coefficients refer to the subscript x in the chemical formula designating the rare earth element. The percentage (for Killick's material) is percentage by weight, according to the labeling approach Killick used. 0.25-percent Ho (Killick) is approximately 0.02 Ho.

by providing heat sinking in the slot (for example, by means of coolant flow through a hollow latching wire). Neither of these approaches was necessary to achieve the required 2-kW average power capability.

Thermal calculations were carried out based on a one-dimensional flow of heat. The geometry used for the cal-

culation is illustrated in Fig. 8. The variations from Fig. 1 make possible the assumption of single dimensional heat flow. Since deviations from single dimensional heat flow lead to a reduction in path lengths, a temperature rise calculated assuming single dimensional heat flow will be greater than the actual temperature will rise and will provide an upper boundary. The calculation in the ferrite assumes a uniform generation of heat throughout the garnet material and based on 0.0327-dB/cm attenuation along the axis of the toroids. The sum of temperature rises due to heat flow through the garnet and beryllia is 9°C. The value of the coefficient of thermal conduction for ferrite and beryllia are 0.0626 and 1.88 W/cm²/cm/°C. The temperature rise due to heat conduction through the ferrite and beryllia are seen to be very small and pose no problem. The temperature rise within the interfaces is probably significantly higher and was not calculated due to the difficulty in accurately specifying the composition of these discontinuities.

Using flux drive, measurements were made of phase shift as a function of temperature and power. The results

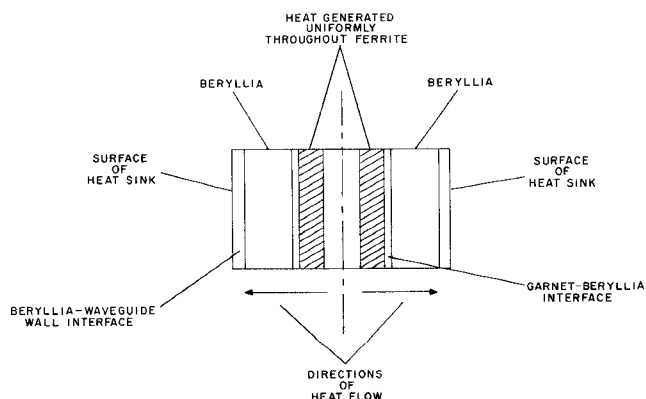


Fig. 8. Geometry used for thermal calculations. The narrow walls are assumed to be the heat sink surfaces to simplify the calculations (which reduces the calculation to a single dimension).

appear in Fig. 9 and, as can be seen, have similar shape responses. No direct comparison is made between these characteristics. By virtue of the similarity of their shapes, it would appear that the sum of the temperature rises from the heat sink to the garnet under power is approximately equivalent to the temperature range over which the garnet was tested versus temperature.

Differential phase shift as a function of average power was monitored during the average power test. The MS3516C material selected through peak power tests was used for this test. Differential phase shift was taken with current drive and flux drive for average powers from 100 to 2000 W. Current drive characteristics were obtained, first with the current drive sufficient to establish full remanent magnetization for each power level. After the current drive data were taken, the flux drive was adjusted so that the phase shift for flux drive was equal to that for current drive for 2000 W average RF power. The phase shift for flux drive was then taken versus power. Results for both drive modes are shown in Fig. 9. The differential phase variation is clearly less for flux drive than for current drive. The total variation for current drive and flux drive were, respectively, $36^\circ (\pm 18^\circ)$ and $11^\circ (\pm 5.5^\circ)$. No effort was made to improve upon these initially observed characteristics.

Differential phase-shift data taken previously on G-500

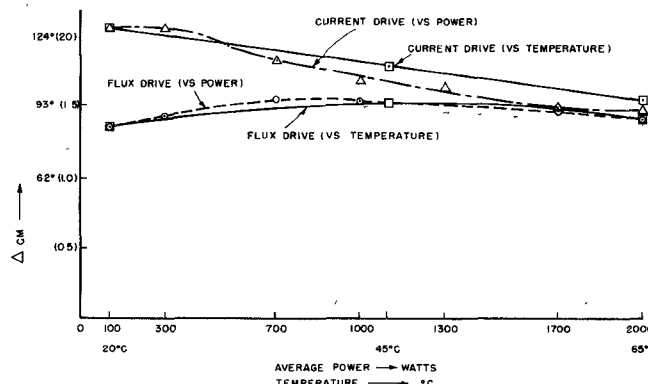


Fig. 9. Differential phase shift versus power and temperature, respectively, for MS3516C and G-500.

(which has a high temperature characteristic similar to MS3516C⁷) are also shown in Fig. 9. The waveguide cross section for the temperature data was identical to that for the high power tests. G-500 was used for the temperature tests as an expedient prior to availability of MS3516C material samples.

No arcing occurred during average power tests which were conducted at a high pulse repetition rate with pulse length comparable to that used during peak power tests.

V. CONCLUSIONS

A high average power garnet toroidal type digital phase shifter has been designed and tested to 2000 W average power, twice the power previously reported for this type device. The tests indicate that a substantially higher average power could be accommodated by the phase-shifter design through incorporation of changes suggested.

The high average power was achieved by fully dielectrically loading the region between the ferrite and waveguide walls with high thermal conductivity beryllia. Phase stability not exceeding $\pm 5^\circ$ for 90° phase shift was achieved by the additional use of flux drive instead of conventional current drive. This configuration was computer programmed for optimization of the phase-shifter characteristics. Curves are given which provide a design basis for this configuration.

REFERENCES

- [1] L. R. Whicker and R. R. Jones, "Design considerations for digital latching ferrite phase shifters," *Microwaves*, Nov. 1966.
- [2] G. P. Rodrigue, J. L. Allen, L. J. Lavedan, and D. R. Taft, "Operating dynamics and performance limitations of ferrite digital phase shifters," *IEEE Trans. Microwave Theory Tech. (1967 Symposium Issue)*, vol. MTT-15, pp. 709-713, Dec. 1967.
- [3] R. A. Stern and J. A. Agrios, "A 500 kW X-band air-cooled ferrite latching switch," in *IEEE MTT Int. Symp. Dig.*
- [4] Trans Tech, Inc., Gaithersburg, Md., catalog.
- [5] J. L. Allen, "The analysis of dielectric loaded ferrite phase shifters including the effects of losses," Ph.D. dissertation, Georgia Inst. Technol., Atlanta, May 1966.
- [6] E. A. Killick, "Problems of materials for high power ferrite phase shifters," in *Proc. Symp. Electrically Scanned Array Techniques and Applications* (Rome, N. Y.), TDR, RADC 64-225, vol. 1, July 1964.
- [7] R. West, Trans. Tech, Inc., Gaithersburg, Md., private communication.